INTL JOURNAL OF ELECTRONICS AND TELECOMMUNICATIONS, 2024, VOL. 70, NO. 4, PP. 915-921
Manuscript received August 06, 2024; revised October 2024. doi: 10.24425/ijet.2024.152078

Efficient Pruned-DFT FBMC-OQAM for Performance Enhancement of MIMO Channel Equalization Techniques

Thamer M. Jamel, and Ali Al-Shuwaili

***Abstract*—A The next generation of wireless systems, like 5G/6G, ought to accommodate a wide range of potential use cases like massive real-time and machine-type communications. Accordingly, such systems need to provide high throughput, low latency, and a low peak to average power ratio (PAPR). It is not feasible to fulfil each of these needs with a single 5G/6G technique. On one hand, MIMO technique can potentially improve spectral efficiency and hence support more date rates. On the other hand, the utilization of multi-carriers' techniques like FBMC/OQAM, or offset quadrature amplitude modulation, offers a compelling substitute for the traditional cyclic prefix-based orthogonal frequency division multiplexing (CP-OFDM) because of its excellent spectral efficiency and extremely low out-of-band radiation. However, the FBMC/OQAM orthogonality constraint is loosened, confined to the real field alone, resulting in intrinsic interference. This interference causes incompatibilities between FBMC/OQAM and certain MIMO schemes. Also, equalizing the time-varying MIMO channel is even more difficult when the complex valued symbol—which includes both real and imaginary FBMC/OQAM task, primarily due to the general non-flatness of the subchannels. From this perspective, we first suggest in this paper an efficient pruned-DFT-based implementation of MIMO to restoring the complex orthogonality and also reduce the complexity of the whole system. Then, we optimize MIMO channel equalization by efficiently separating and equalizing multiple parallel channels using various equalization techniques. The numerical results, presented as MSE versus subcarrier index, show that Pruned DFT technique consistently achieves lower MSE values compared to the standard MIMO FBMC-OQAM across various configurations, which indicates better error performance and its robustness in dynamic channel conditions.**

***Keywords*—FBMC-OQAM; MIMO; equalization; MSE; pruned DFT**

I. INTRODUCTION

THE 5G and beyond wireless communication systems need to have low computational complexity and high spectral efficiency. They also need to provide high throughput, low latency, and a low peak to average power ratio (PAPR). It is not feasible to fulfill each of these needs with a single state-of-the-art technique like MIMO or FBMC. As a result, Filter Bank Multicarrier (FBMC), is developed and is primarily used to filter the desired signal. The utilization of FBMC/OQAM, or offset quadrature amplitude modulation, offers a compelling substitute for the traditional cyclic prefix-based orthogonal frequency division multiplexing (CP-OFDM) particularly in terms of high bandwidth efficiency and enhanced resistance to Doppler spread and frequency offset [1-3]. Under realistic highly dispersive and frequency-selective channels, Intercarrier Interference (ICI) and inter-Symbol Interference (ISI) lead to high complexity, high Peak to Average Power (PAPR), and high out of band (OOB) leakage at the receiver [4, 5]. Accordingly, a technique known as pruned DFT spread FBMC has been proposed in the literature to mitigate the PAPR among various subcarriers [6]. Nevertheless, channel equalization in Equalizing the channel in multiple-antenna (MIMO) time-varying systems becomes even more difficult when the complex valued symbol—which includes both real and imaginary FBMC/OQAM is a challenging task, primarily due to the general non-flatness of the subchannels [7, 8].

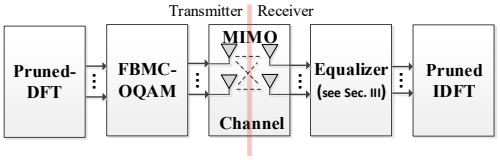

Fig.1. Block diagram of the proposed pruned-DFT FBMC-OQAM with MIMO channel equalization

The next generation of wireless systems, i.e., 5G/6G and beyond, ought to accommodate a wide range of resource-demanding services, such as massive Machine-Type Communication (mMTC) or Ultra Reliable and low latency communication (URLLC) [9]. Instead of focusing on the MIMO scenario, this work suggests implementing a parallel multi-stage processing architecture on both ends of the communication link. Because of its excellent spectral efficiency and extremely low out-of-band radiation, FBMC is regarded as a promising non-orthogonal waveform However, the FBMC/OQAM orthogonality constraint is loosened, confined to the real field alone, resulting in intrinsic interference. The presence of this interference causes incompatibilities between FBMC-OQAM and certain popular multiple-input multiple-output (MIMO) schemes. From this perspective, we propose in this paper an effective FBMC-OQAM implementation based on pruned spreading to enable applying MIMO with pruned-DFT FBMC-OQAM by restoring the complex orthogonality. The input

First Author is with Department of Communications Engineering, University of Technology, Baghdad, Iraq (e-mail: thamer.m.jamel@uotechnology.edu.iq).

Second Author is with College of Engineering, University of Information Technology and Communications, Baghdad, Iraq (e-mail: ali.najdi@uoitc.edu.iq).

signal divides the band-pass filter array into several parts. The components recombine the altered version of the original signal after being attenuated differently. Symbols are sent over a rectangular time-frequency grid in such a multicarrier system. The shape in frequency and, thus, in time, are determined by the subcarrier spacing. While a small subcarrier spacing boosts bandwidth efficiency, a high subcarrier spacing enables low latency transmissions. Additionally, varying subcarrier spacings enable the transmission system to adapt to channel conditions.

In the ever-evolving landscape of wireless communication, addressing the challenges posed by increasing demand for higher data rates, improved spectral efficiency, and interference mitigation is imperative. This research paper is a deep dive into the intricacies of a specific communication framework—Multiple Input Multiple Output (MIMO) systems embedded in the context of Filter Bank Multicarrier Offset Quadrature Amplitude Modulation (FBMC-OQAM).

The essence of this study lies in its ambition to dissect and critically evaluate various equalization techniques deployed within MIMO FBMC-OQAM systems. MIMO systems, known for their capacity to exploit spatial diversity, combined with the unique characteristics of FBMC-OQAM modulation, form a complex communication paradigm. As such, our research endeavours to unravel the nuances of equalization strategies, investigating their impact on system performance in diverse scenarios.

Through meticulous examination and comparative analysis, we aim to provide a comprehensive understanding of the strengths and weaknesses inherent in different equalization approaches. The goal is to identify and elucidate the most effective equalization strategies, shedding light on their applicability and adaptability in optimizing the performance of MIMO FBMC-OQAM systems. This research contributes to the academic discourse on advanced communication systems and holds practical implications for the ongoing evolution of wireless communication technologies.

II. RELATED WORK

The work in [10] analyzes the BER performance of the MIMO OFDM system for AWGN Channel, Rayleigh Fading Channel along with a simulation channel using different modulation techniques. Also, the result of the analysis suggests a better technique to improve the BER characteristic of the MIMO-OFDM system. In [11], design of the OFDM system transmitter and receiver is introduced and Simulation is done using MATLAB. Bit Error Rate performance of BPSK modulation and OFDM -BPSK System over Rayleigh fading channel is analyzed in [12]. The simulation results show that the simulated bit error rate is in good agreement with the theoretical bit error rate for BPSK modulation. Reference [13] suggests a new method to mitigate the effect of Inter-Carrier Interference (ICI) in FFT-based multicarrier systems and compares it to a Discrete Cosine Transform (DCT)-based system in terms of bit error rate. The proposed ICI-cancellation technique provides enhanced BER performance compared to other self-cancellation techniques. The authors in [14] propose a hybrid modulation scheme that is composed of two techniques: FBMC-OQAM and single-carrier frequency-division multiple access (SC-FDMA). Besides the classical FBMC system, they augment the proposed design with pruned-DFT in combination with one-tap scaling. The hybrid scheme is cyclic prefix free, enjoys less power consumption and allows low latency transmissions. A comparison of the BER performance of different modulation schemes like, QPSK and 16-QAM, and various equalization techniques such as constant modulus algorithm and maximum likelihood sequence estimate for the AWGN and Rayleigh fading channels is performed in [15]. Among the considered digital modulation schemes, BPSK is showing better performance as compared to QPSK and 16-QAM. The study referenced in [16] introduced an efficient method for implementing FBMC/OQAM using block spreading to reestablish complex orthogonality, facilitating the use of MIMO with FBMC/OQAM. This method employs a discrete Haar transform to achieve low computational complexity. The effectiveness of the proposed methods was analyzed and compared to CP-OFDM across three MIMO schemes: space-time block coding Alamouti schemes, spatial multiplexing with zero-forcing, and maximum likelihood detection schemes. Simulation results indicate that the proposed methods allow the application of MIMO schemes with FBMC, delivering performance and complexity comparable to CP-OFDM. To further enhance the amount of PAPR reduction, the authors in [17] proposed a pre-coding method based on a pruned DFT in combination with one-tap scaling. The proposed technique is compared with FBMC-OQAM and SC-FBMC. They applied the Firefly optimization algorithm to prune the DFT spread and swarm intelligence concept. The results show that the implemented technique i.e., FA-Pruned DFT spread has good PAPR, spectral efficiency and lower latency. Some other work considers the equalization stage or/and chromatic dispersion in FBMC-OQAM for SISO channel only [18-28]. A set of equalization techniques like frequency spreading and frequency sampling is implemented and compared for FBMC-OQAM with pruned DFT. In addition to equalization, the work in [19] extends the original work of [18] by considering also the channel estimation technique. Using Pilot Symbol Aided Channel Estimation (PSACE) improves the overall error performance of considered system. The related method of adaptive maximum likelihood algorithm for FBMC-OQAM in fiber optic systems is used in [20] to optimize chromatic dispersion compensation. Finally, BER performance of various equalization techniques, including single-tab equalizer and frequency spreading, is investigated in [21-28] for FBMC-OQAM and without the inclusion of pruned-DFT method.

III. METHODOLOGY

In this first part of this section, we introduce the basic formulation of the considered system model including our main metric in this study, i.e., MSE. Then, in subsection B, we elaborate on the formulation of different equalization techniques integrated into the system model and used in the upcoming numerical results.

A. System model

We consider a MIMO-FBMC/OQAM system with the number of transmit and receiver antenna is denoted as Nt and Nr, respectively. A simplified block diagram of the considered system model is shown in Figure 2. The system has M subcarriers with spatial multiplexing is used for the sake of sending independent stream of symbols over different antennas.

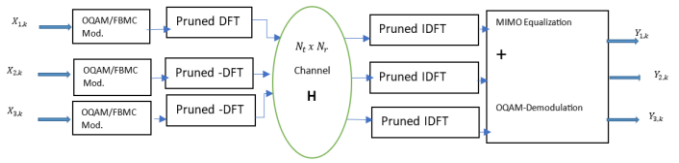

Fig.2. Transmitter-receiver structure of the proposed scheme

The complex input symbol sequence to be transmitted on the k-th subchannel over the i-th transmit antenna is denoted as s_{ki}. These symbols are OQAM modulated at the input of the synthesis filter. We assume that the MIMO channel is time-invariant, and the m-th tap of the channel impulse response (CIR) between the i-th transmit antenna and the j-th receive antenna is denoted as $h_{ij}(m)$. All channels are assumed to be the same length. The received signal at the j-th receive antenna reads :

$$y_j(t) = \sum_{i=1}^{N_t} \sum_{m=0}^{L-1} h_{ij}(m) s_i\,(t - \tau_m) + w_j(t) \quad (1)$$

where $s_i(t)$ is the transmitted signal from the i-th transmit antenna; τ_m represents the delay associated with the m-th tap; finally, $w_j(t)$ is the additive white Gaussian noise (AWGN) at the j-th receive antenna. Using the compact matrix notation, the received signal in the frequency domain after demodulation and equalization $\boldsymbol{Y}$ is given as :

$$\boldsymbol{Y} = \boldsymbol{X}\boldsymbol{H} + \boldsymbol{W} \quad (2)$$

With $\boldsymbol{X}$ being the transmitted signal over a channel with matrix $\boldsymbol{H}$ and noise captured in vector $\boldsymbol{W}$.

The pruned DFT reduces the complexity by eliminating redundant calculations. The system model leverages this by focusing on the essential subcarriers. The LS channel estimation in the frequency domain is therefore reads :

$$\boldsymbol{H}_{LS} = \boldsymbol{U}\boldsymbol{h} + \boldsymbol{W} \quad (3)$$

Where we defined matrix $[U]_{m,n} = e^{-j2\pi n[\psi]_m/N}$ over $m = 0, 1, \dots, P-1$ and $n = 0, 1, \dots, L-1$ with $\boldsymbol{h} = [h_0, h_1, \dots, h_{L-1}]^{\boldsymbol{T}}$ being a vector of channel tabs. The extended channel response $\boldsymbol{H}_N$ is padded to match the size of the signal:

$$\boldsymbol{H}_N = [\boldsymbol{H}_1 : \boldsymbol{H}_{LS} : \boldsymbol{H}_r] \quad (4)$$

where $\boldsymbol{H}_1$ and $\boldsymbol{H}_r$ are the parts of the channel response outside the pilot subcarriers. Then, the estimated channel response is :

$$\widehat{\boldsymbol{H}} = \boldsymbol{U}\widehat{\boldsymbol{h}} \quad (5)$$

Where $\widehat{\boldsymbol{h}} = \boldsymbol{U}_N^H \widehat{H}_N / N$ and $(.)^H$ denotes the Hermitian transpose of a matrix. Note that, in this case, the matrix $\boldsymbol{U}$ is resized as :

$$[U_N]_{m,n} = e^{\frac{-j2\pi n\left(m-\frac{N}{2}\right)}{N}}, \quad m = 0, 1 \dots, N-1 \quad \text{and} \quad n = 0, 1, \dots, L-1 \quad (6)$$

The normalized mean square error (NMSE) performance is given by:

$$\Gamma = \frac{1}{P}\mathrm{tr}(\mathbb{E}\left[(\widehat{\boldsymbol{H}} - \widehat{\boldsymbol{H}})(\widehat{\boldsymbol{H}} - \widehat{\boldsymbol{H}})^H\right])$$

$$= \frac{\sigma^2}{PN^2}\mathrm{tr}(\boldsymbol{U}\boldsymbol{U}^H\boldsymbol{U}\boldsymbol{U}^H) + \frac{1}{PN^2}\mathrm{tr}(\boldsymbol{D}\boldsymbol{\Phi}\boldsymbol{D}^H) \quad (7)$$

Where tr(.) denotes the trace of a matrix; $\boldsymbol{D} = \boldsymbol{U}\boldsymbol{U}^H$; $\boldsymbol{\Phi} = E[(\widehat{\boldsymbol{H}}_\Omega - \boldsymbol{H}_\Omega)(\widehat{\boldsymbol{H}} - \boldsymbol{H}_\Omega)^H]$, and σ^2 is the noise variance.

B. *MIMO equalization*

The equalization for MIMO FBMC-OQAM is carried out in the frequency domain. All subchannels between each transmit and receive antenna are approximated by a single tap. Therefore, for each subchannel the system can be considered as a MIMO frequency flat channel and the equalizer is a simple single-tab equalizer. In this section, we first consider the benchmark single-tab, or one-tab, equalizer and then we proceed to discuss more advanced equalization techniques.

1) *One-tab MMSE equalizer*

The one-tab Minimum Mean Squared Error (MMSE) equalizer is given by

$$e_{i_n} = \gamma \frac{g_{i_n}^*}{|g_{i_n}|^2 + P_{noise}} \quad (8)$$

where the one-tab channel is represented by g_{i_n}, and γ is a scaling factor that ensures impartial equalization [14]. the phrase $e_{in} \in C^{I\times 1}$ refers to a group of equalizer elements that are utilized to obtain the equalized signal. In closing, it is important to note that the equalizer in (x) for noiseless (i.e., $P_{noise} = 0$) or time-invariant channels may be simplified to Zero Forcing (ZF) equalizer, or $e_{i_n} = \frac{1}{g_{i_n}}$.

2) *Frequency Sampling Equalizer (FSE)*

By using frequency sampling to obtain the frequency response (FS) of each subchannel, this sturdy multi-tab structure enables per-subchannel equalization. To analyze the coefficient of one-tap equalizer in detail, the FS sampled with frequency points is obtained first, and each point corresponds to a coefficient that is utilized to equalize a specific subchannel. Next, the FS of single-tap equalizers is interpolated to get the multi-tab function. The equalized signal with an L-tab frequency sampling equalizer is derived and may be expressed as [29]:

$$\widetilde{y_n} = \sum_{l=0}^{L} w(l)\, y_n(i-l) \quad (9)$$

Where $w(l)$ is the L equalization coefficients, which are produced by multiplying the IFFT matrix by coefficients derived from the previously mentioned interpolation.

3) *Parallel Analysis Filter Bank (PAFB) Equalizer*

It is recommended in [30] to employ numerous AFBs to create a parallel equalization system that can extract symbols without distortion. The suggested equalizer's performance is calculated asymptotically, or on the assumption that the FBMC systems have a high number of carriers. In [30, Theorem 1], it is demonstrated analytically that the signal recovered using this equalization may be expressed as follows:

$$\widetilde{y_n} = y_n - (2I)^{-L}\, d_n^L + o\,(I^{-L}). \quad (10)$$

A matrix whose members approach zero as $I \to \infty$. is indicated by the expression $o\,(I^{-L})$. This equation means that the transmitted signal may be recovered by the PAFB equalizer

(with L parallel single-tab stages) up to a distortion of order I^{-L}, where the distortion function is defined using the real and imaginary components of the equalized signal [30]

$$d_n^L = Re\,\{D_{odd}(p,q)\} + j\,Im\{D_{even}(p,q)\} \quad (11)$$

Whereas the two parameters, p and q , constitute the prototype filter, D_{odd} and D_{even} are specified in the proof of Theorem 1 in [10].

4) Frequency Spreading Equalizer

By increasing each subcarrier's bandwidth and lowering the time-domain prototype filter length in the FBMC system, this equalization mechanism operates [31]. As a result, in the frequency domain where the number of subcarriers exactly equals the number of non-zero samples of the prototype filter, the transmitted data is dispersed over a certain number of subcarriers. The frequency spreading equalizer's weight coefficient in formula is:

$$w(i) = \frac{1}{F(i)}\ , 0 \le i \le IQ - 1, \quad (12)$$

As previously, we defined I as the total number of subcarriers, which is distributed by factor Q in this instance [31].

5) Overlap and Save Equalizers

Discrete convolution between lengthy sequences may be efficiently performed using overlap and save, which involves assessing a smaller portion of the original sequence first and concatenating the segments together [32]. This technique was used in the work in [33] to offset some of the deficiencies in the OFDM modulated optical fiber system. We expand on their work by adding pruned FBMC-OQAM system overlap and save-based equalization. To this end, the weight coefficient vector in this case is:

$$w = S_x F^*(FS_xF^* + \gamma S_n)^{-1} \quad (13)$$

Where $S_x \overset{\text{def}}{=} E[x_n x_n^*]$ is the Power Spectral Density (PSD) matrix of the transmitted symbols and similarly S_n denotes the noise PSD. In [26], the power cost resulting from the usage of CP has been reflected by scaling the noise PSD by γ. Instead, we normally specify γ=1 for FBMC here. The P-FBMC-OQAM receiver uses the equalization procedures described in this part,

IV. RESULTS AND DISCUSSION

In this section, we aim to assess the performance of several equalization techniques for pruned-DFT MIMO under different types of channel models and different number of subcarriers as detailed next. We dedicate section A to the results obtained with Pedestrian A channel model (ITU-PedA) that is characterized by delays=1e-9*[0 110 190 410]; and powers=[0 -9.7 -19.2 -22.8]; whereas Sec.B shows the results obtained with Vehicular A channel (ITU-VehA) model (at speed of 60 km/hr) having power of delay profile as delays=1e-9*[0 300 700 1100 1700 2500] and powers=[0 -1 -9 -10 -15 -20]. The full list of simulation parameters is shown in Table I.

For clear presentation, we divide the results presented in this section into two parts where each part corresponds to the results obtained under one of the two channels considered in the simulations (see Table I).

In all figures, we consider the benchmark one-tab MMSE equalizer, termed as "1-tab" and compare its performance to the following proposed set of equalization techniques (cf. Sec. III): (i) "3-tab F. Sampling": refers to the frequency sampling equalizer with three tabs (and similarly for another instance of this equalizer but with seven tabs instead); (ii) "AFBs Two Parallel": refers to the AFB equalizer with two parallel stages (and similarly for another instance of this equalizer but with three parallel stages); (iii) "F. Spreading": refers to frequency spreading equalizer; (iv) "Overlap & Save": refers to overlap-and-save-based equalizer. All formulation related to these types are presented in Sec. III.

TABLE I
SIMULATION PARAMETERS

Parameter	Value
Number of symbols	1000
Number of transmit antennas	2
Number of receive antennas	4
symbol period [s]	1/15e3 [s]
Es/No	45
Number of subcarriers	128 , 256
Sampling rate	504000 Hz
Overlapping factor	4
Criterion for equalizer	'MMSE'
Center Frequency [Hz]	1e9
PAM modulation order	4

A. MSE performance under Channel #1

To grasp the equalization performance of the proposed pruned-DFT MIMO FBMC-OQAM system, let us first have a look at the Channel #1 frequency response at the receiving side which is depicted in Figure. 3. It is evident that the channel exhibits a sinusoidal-like response in this case. Under this channel with128 subcarriers, the MSE performance vs. the subcarriers number of the system under study is shown in Figure. 4. The plot indicates that across the subcarrier index, the MSE for standard MIMO FBMC-OQAM fluctuates around -49 dB, while the Pruned DFT technique consistently achieves a lower MSE, approximately -53 dB. The Pruned DFT method shows more consistent MSE values across subcarriers compared to the standard technique, suggesting better equalization performance which is a direct consequence of the amount of complexity reduced when pruned-DFT is integrated into the system structure compared to the conventional MIMO FBMC. It is worth mentioning here that all techniques shown try to equalize the channel by inversing its frequency response. However, the most successful, i.e., with minimum MSE, is the FS equalizer. We will provide a more in-depth numerical comparison at the end of this section. Similar observation is also applied to the case with 256 subcarriers with the note that here the MSE is at a higher level due to the denser constellation on frequency-time grid and hence more error-prone equalization as illustrated in Figure 5.

To have a closer look at the result displayed in Figure 4, we now provide numerical comparison for the performance of the same set of equalizers shown in that figure. Table II lists the average values of MIMO MSE for the case of 128 subcarriers under Channel #1 for both the conventional and the DFT-enhanced FBMC.

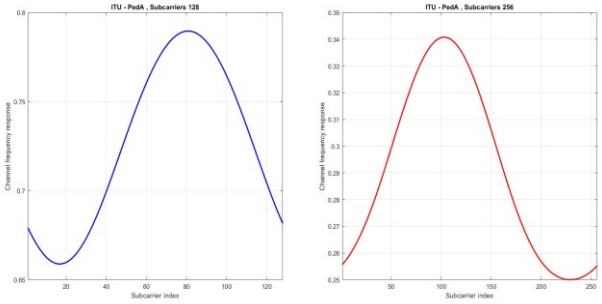

Fig.3. Channel #1 frequency response of ITU-PedA at receiver side : 128 subcarriers; and 256 subcarriers

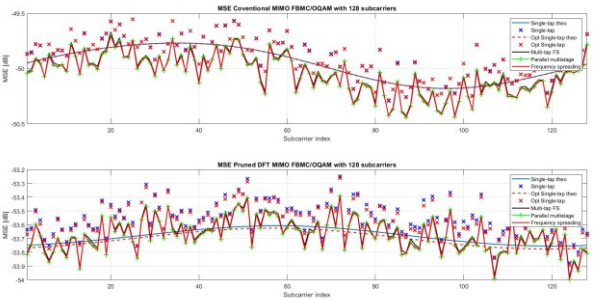

Figure 4. MSE performance vs. subcarriers count of MIMO equalization with 128 subcarriers under Channel #1 without and with Pruned DFT

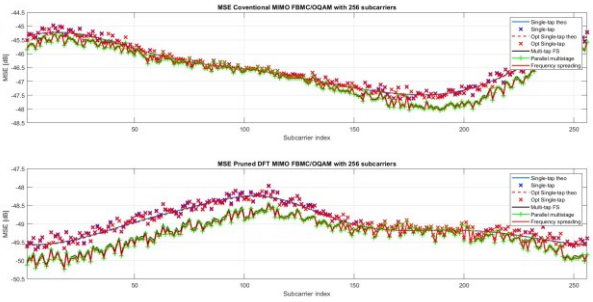

Figure 5. MSE performance vs. subcarriers count of MIMO equalization with 256 subcarriers under Channel #1 without and with Pruned DFT

The data in Table II reveals that Pruned DFT MIMO FBMC/OQAM has consistently lower MSE values compared to MIMO FBMC/OQAM, indicating better performance in terms of error reduction.

In both setups, the MSE_Parallel_multistage and MSE_frequency_spreading techniques offer the best MSE performance. The MSE values for MSE_theo_approx and MSE_theo_approx_opt are very close, indicating that the theoretical approximation is well aligned with the optimal values.

TABLE II
AVERAGE MSE PERFORMANCE OF MIMO EQUALIZERS WITH 128 SUBCARRIERS UNDER CHANNEL #1

Technique	MSE value (conventional)	MSE value (pruned-DFT)
MSE_theo_approx	-49.9602	-53.6817
MSEConventional_single_ tap_equalizer	-49.9030	-53.5469
MSE_theo_approx_opt	-49.9617	-53.7007
MSE_opt	-49.9041	-53.5651
MSE_MultiTapFS	-50.0431	-53.6655
MSE_Parallel_multistage	-50.0556	-53.6772
MSE_frequency_spreading	-50.0556	-53.6770

The differences between MSE_theo_approx and MSEConventional_single_tap_equalizer and between MSE_theo_approx_opt and MSE_opt are marginally better in the Pruned DFT MIMO FBMC/OQAM scenario. The Pruned DFT MIMO FBMC/OQAM technique shows better MSE performance across all equalization methods compared to the conventional MIMO FBMC/OQAM, making it a more effective approach for error minimization in a multipath fading environment modeled by Channel #1, i.e., ITU-Ped A.

B. MSE performance under Channel #2

We now turn to the case where the performance is tested assuming ITU- VehA channel model operated at 60 km/hr. The frequency response of this channel is shown in Figure 6 for two considered numbers of subcarriers. With 128 subcarriers, we can observe that the pruned-DFT-based equalization brings superior performance, especially with FS frequency spreading equalizer. This can be easily obtained from the MSE performance plotted in Figure 7, where FS equalizer actively tracking the variation of the channel leading to achieve the lowest MSE compared to other techniques. The Pruned DFT method demonstrates greater robustness in the presence of higher Doppler effects, as indicated by its lower and more stable MSE values.

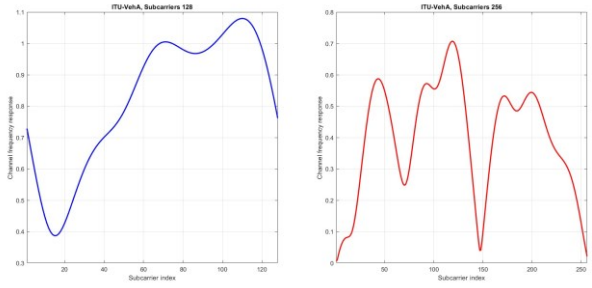

Fig. 6. Channel #2 frequency response: (a) 128 subcarriers; (b) 256 subcarriers

With reference to Figure 8 where 256 subcarriers is used in with Channel #2 channel model, the MSE performance for standard MIMO FBMC-OQAM and Pruned DFT MIMO FBMC-OQAM

is again evaluated. MSE Performance: The results also demonstrate that the MSE for standard MIMO FBMC-OQAM varies around -48 dB, while the Pruned DFT technique achieves lower and more stable MSE values around -54 dB across the subcarrier indices. The results also confirm that the Pruned DFT technique scales better with the increased number of subcarriers, maintaining lower MSE values.

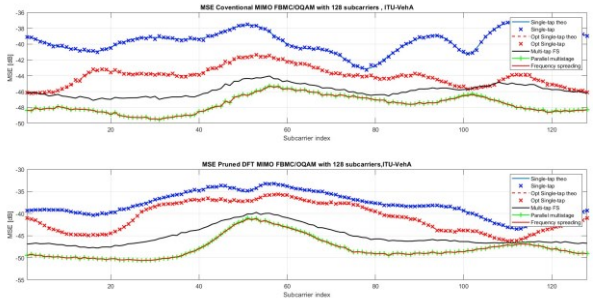

Fig.7. MSE performance vs. subcarriers count of MIMO equalization with 128 subcarriers under Channel #2: without and with Pruned DFT

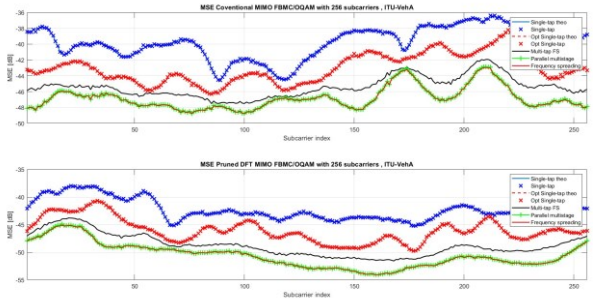

Fig.8. MSE performance vs. subcarriers count of MIMO equalization with 256 subcarriers under Channel #2: without and with Pruned DFT.

To shed more light on the performance gain obtained in the previous figure, we now provide more in-depth numerical comparison for both the conventional and pruned-DFT-enhanced MIMO equalization in FBMC-OQAM. Under Channel #2 model with 256 subcarriers, the steady-state values of MSE performance in depicted in Figure 9. The results here confirm again the benefit of applying pruned-DFT-based equalization in MIMO configuration in terms of MSE. As a final note, the combination of a higher number of subcarriers and a dynamic vehicular channel highlights the effectiveness of the Pruned DFT technique in maintaining lower MSE values under challenging conditions of vehicular environment.

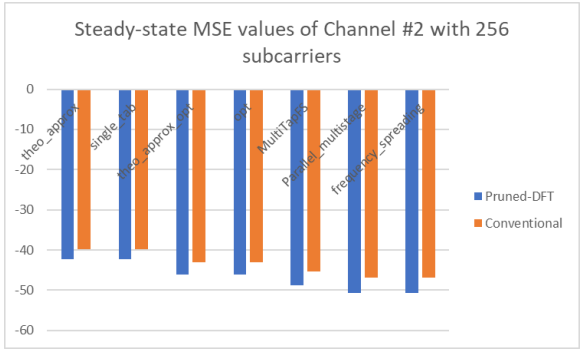

Fig.9. Numerical comparison of MSE values for MIMO equalizers under Channel #2 with 256 subcarriers

V. CONCLUSIONS

The pruned-DFT technique, incorporated into MIMO FBMC-OQAM, shows greater consistency and stability in MSE values across different subcarrier indices. This consistency is particularly notable in the ITU Veh A model, where the pruned-DFT technique maintains lower MSE values even under higher Doppler effects, demonstrating its robustness in dynamic channel conditions. The numerical results, presented as MSE versus subcarrier index, underscore several critical aspects of the equalization techniques. The Pruned DFT technique consistently achieves lower MSE values compared to the standard MIMO FBMC-OQAM across various configurations, which indicates better error performance. For example, in the ITU Pred A model with 128 subcarriers, the Pruned DFT technique achieves an MSE of approximately 25% better compared for the standard method. Overall, the results provide a comprehensive comparison of the MSE performance of standard and Pruned DFT MIMO FBMC-OQAM techniques. The findings highlight the computational efficiency, scalability, and enhanced performance of Pruned DFT techniques, making them a viable choice for practical MIMO system applications.

REFERENCES

[1] Lawrence and S. V. George, “Pruned DFT Spread FBMC,” vol. 15, no. 2, pp. 8–11, https://doi.org/10.9790/2834-1502010811

[2] M. Agrawal, S. Singh, N. Raisen, R. Bhopal, and Y. Raut, “BER Analysis of MIMO OFDM System for AWGN & Rayleigh Fading Channel,” 2011.

[3] S. S. Ghorpade and S. V Sankpal, “Behaviour of OFDM System using MATLAB Simulation,” 2013.

[4] M. Divya, “Bit Error Rate Performance of BPSK Modulation and OFDM-BPSK with Rayleigh Multipath Channel,” Int J Eng Adv Technol, 2013, [Online]. Available: www.ijeat.org

[5] S. Gupta, U. Dalal, and V. N. Mishra, “Performance on ICI Self-Cancellation in FFT-OFDM and DCT-OFDM System,” Journal of Function Spaces, vol. 2015, 2015, https://doi.org/10.1155/2015/854753

[6] R. Nissel and M. Rupp, “Pruned DFT-Spread FBMC: Low PAPR, low latency, high spectral efficiency,” IEEE Transactions on Communications, vol. 66, no. 10, pp. 4811–4825, Oct. 2018, https://doi.org/10.1109/TCOMM.2018.2837130

[7] T. M Jamel, A. Al-Shuwaili, and B. M Mansoor, “Novelty Study of the Window Length Effects on the Adaptive Beam-forming Based-FEDS Approach,” International Journal of Computing and Digital Systems, vol. 9, no. 6, pp. 1221–1227, 2020.

[8] Al-Shuwaili, M. Dh Hassib, and T. M Jamel, “Ball’s-Based Adaptive Channel Estimation Scheme Using RLS Family-Types Algorithms,” International Journal of Computing and Digital Systems, vol. 12, no. 1, pp. 469–477, 2022.

[9] N. Al-Shuwaili, A. Bagheri and O. Simeone, "Joint uplink/downlink and offloading optimization for mobile cloud computing with limited backhaul," 2016 Annual Conference on Information Science and Systems (CISS), Princeton, NJ, USA, 2016, pp. 424-429.

[10] M. Agrawal, S. Singh, N. Raisen, R. Bhopal, and Y. Raut, “BER Analysis of MIMO OFDM System for AWGN & Rayleigh Fading Channel,” 2011.

[11] S. S. Ghorpade and S. V Sankpal, “Behaviour of OFDM System using MATLAB Simulation,” 2013.

[12] M. Divya, “Bit Error Rate Performance of BPSK Modulation and OFDM-BPSK with Rayleigh Multipath Channel,” Int J Eng Adv Technol, 2013, [Online]. Available: www.ijeat.org

[13] S. Gupta, U. Dalal, and V. N. Mishra, “Performance on ICI Self-Cancellation in FFT-OFDM and DCT-OFDM System,” Journal of Function Spaces, vol. 2015, 2015, https://doi.org/10.1155/2015/854753

[14] R. Nissel and M. Rupp, “Pruned DFT-Spread FBMC: Low PAPR, low latency, high spectral efficiency,” IEEE Transactions on Communications, vol. 66, no. 10, pp. 4811–4825, Oct. 2018, https://doi.org/10.1109/TCOMM.2018.2837130

[15] Md. F. Ahmed, Md. F. Ahmed, and A. Z. Md. Touhidul Islam, "Comparison of Bit Error Rate Performance of Various Digital Modulation Schemes over AWGN and Rayleigh Fading Channels using Simulink," The International Journal of Ambient Systems and Applications, vol. 9, no. 2, pp. 7–16, Jun. 2021, https://doi.org/10.5121/ijasa.2021.9202

[16] Walid ali raslan, M. Abdel-Azim Mohamed, and H. Mohamed Abdel-Atty, "Article 7 2022 Part of the Signal Processing Commons, and the Systems and Communications Commons Recommended Citation Recommended Citation raslan," 2022.

[17] K. Naga Bhavani, A. Gangadhar, and M. Hema, "Issue 6 www.jetir.org (ISSN-2349-5162)," 2022. [Online]. Available: www.jetir.org

[18] S. Al-Doori, A. Al-Shuwaili and T. M. Jamel, "Efficient FBMC-OQAM Channel Equalization Through Pruned DFT," 2023 16th International Conference on Developments in eSystems Engineering (DeSE), Istanbul, Turkiye, 2023, pp. 1-6,
https://doi.org/10.1109/DeSE60595.2023.10469207

[19] T. M. Jamel, A. Al-Shuwaili and V. K. Saad, "Performance Analysis of Pilot-Symbol Aided Channel Estimation (PSACE) in FBMC-OQAM System," 2024 21st International Multi-Conference on Systems, Signals & Devices (SSD), Erbil, Iraq, 2024, pp. 1-9,
https://doi.org/10.1109/SSD61670.2024.10549368

[20] Muntadher T Al-Mashkoor, Thamer M Jamel, Haydar M Al-Tamimi, "Optimizing chromatic dispersion compensation using the adaptive maximum likelihood algorithm for FBMC-OQAM fiber optic systems", AIP Conference Proceedings, 2024 , https://doi.org/10.1063/5.0205980

[21] OF Kadhem, TM Jamel, HF Khazaal," Equalization methods for Filter Bank Multicarrier OQAM", Wasit Journal of Engineering Sciences, 2023 , Volume 11, Issue 3, Pages 106-119.

[22] OF Kadhem, TM Jamel, HF Khazaal," Equalization methods for Filter Bank Multicarrier OQAM", Wasit Journal of Engineering Sciences, 2023 , Volume 11, Issue 3, Pages 106-119.

[23] H. A. Fadel and T. M. Jamel, "Evaluating the Performance of 5G Modulation and Beyond: A Review Study," 2024 21st International Multi-Conference on Systems, Signals & Devices (SSD), Erbil, Iraq, 2024, pp. 727-734, https://doi.org/10.1109/SSD61670.2024.10548506

[24] Muntadher T Al-Mashkoor, Thamer M Jamel, Haydar M Al-Tamimi, " Optimizing chromatic dispersion compensation using the adaptive maximum likelihood algorithm for FBMC-OQAM fiber optic systems", AIP Conference Proceedings, 2024 , https://doi.org/10.1063/5.0205980

[25] Abd-Alhussein, M.T., Jamel, T.M., Abdulhadi, H.M. et al. Performance study of the compensations dispersion systems for an optical filter bank multicarrier transceivers technique. J Opt (2024). https://doi.org/10.1007/s12596-024-02055-x

[26] Ahmed H. Abbas, Thamer M. Jamel, " Compensating Chromatic Dispersion and Phase Noise using Parallel AFB-MBPS For FBMC-OQAM Optical Communication System ", International Journal of Electrical and Computer Engineering Systems (IJECES) , Vol. 14 No. 8 (2023), pp 853-867

[27] OF Kadhem, TM Jamel, HF Khazaal," An overview for channel equalization techniques in filter bank', The Second International Conference on Advanced Computer Applications (ACA2023) by Imam Al-Kadhum College, Maysan Departments, Maysan, Iraq. Technically sponsored by IEEE \ Iraq Section

[28] Jamel, Thamer & Alshameri, Ahmed & Mohammed, H. (2023). A Review of Phase Noise Compensation Techniques in Optical Fiber Systems Based-on Filter Bank Multi-Carrier. July 2023, Conference: 1st International Conference on Sustainability System Development (ICSSD2023) , at Erbil, Iraq, 2023, Erbil , Iraq

[29] d Ihalainen, T., Hidalgo Stitz, T., Rinne, M. et al. "Channel Equalization in Filter Bank Based Multicarrier Modulation for Wireless Communications." EURASIP J. Adv. Signal Process. 2007, 049389 (2006). https://doi.org/10.1155/2007/49389

[30] X. Mestre, M. Majoral and S. Pfletschinger, "An Asymptotic Approach to Parallel Equalization of Filter Bank Based Multicarrier Signals," in IEEE Transactions on Signal Processing, vol. 61, no. 14, pp. 3592-3606, July15, 2013, https://doi.org/10.1109/TSP.2013.2261297

[31] M. Bellanger, "FS-FBMC: An alternative scheme for filter bank based multicarrier transmission," 2012 5th International Symposium on Communications, Control and Signal Processing, Rome, Italy, 2012, pp. 1-4, https://doi.org/10.1109/ISCCSP.2012.6217776

[32] V. Oppenheim and R. W. Schafer, Discrete-Time Signal Processing. Upper Saddle River, NJ: Prentice-Hall

[33] E. M. Ip and J. M. Kahn, "Fiber Impairment Compensation Using Coherent Detection and Digital Signal Processing," in Journal of Lightwave Technology, vol. 28, no. 4, pp. 502-519, Feb.15, 2010, https://doi.org/10.1109/JLT.2009.2028245